Materials Science Forum Vol. 815 (2015) pp 412-423

doi:10.4028/www.scientific.net/MSF.815.412

Matrix Elasticity Affects Integrin Expression in Human Umbilical Cord-derived Mesenchymal Stem Cells

Hongwei Lv[1, 2, a#], Yin Zhang[1, 2, b#], Meiyu Sun[1], Jiahui Yang[1], Zhishen Chen[1, 2], Mingming Fan[1], Lisha Li[1, c*] and Yulin Li[1, d*]

[1]The Key Laboratory of Pathobiology, Ministry of Education, Norman Bethune College of Medicine, Jilin University, Changchun 130021, China.

[2]College of Public Health, Jilin University, Changchun 130021, China.

[a]lvhw1013@gmail.com, [b]meizhilinxi@gmail.com, [c]lilisha@jlu.edu.cn, [d]ylli@jlu.edu.cn.
[#]These authors contributed equally to this study and share first authorship.

Keywords: Matrix elasticity, Integrin, Human mesenchymal stem cells (MSCs).

Abstract. Mesenchymal stem cells (MSCs) are a powerful cellular alternative for regenerative medicine and tissue engineering applications due to their multipotency. It is becoming increasingly clear that elasticity of extracellular matrix (ECM) has a profound effect on cell phenotype including adhesion, proliferation and differentiation. Integrins are considered to be important mechanoreceptors in mechanotransduction. While numerous studies have focused on α2, β1 and β3 integrin involvement in substrate stiffness-driven commitment of bone marrow MSCs, comparatively little is known about the change of α5β1 integrin expression in human umbilical cord-derived mesenchymal stem cells (hUCMSCs) on substrates of variable stiffness. We plated hUCMSCs on fibronectin coated polyacrylamide hydrogels with elasticity corresponding to Young's modulus ranging from 3 to 65 kPa. Our results showed that hUCMSCs displayed different morphologies on substrates of varying stiffness. Cells led to branched morphology similar to that of nerve cells when cultured on soft matrices, while cells became more spread and presented polygonal shapes on stiff substrates. Furthermore, hUCMSCs expressed α5 integrin both on soft substrates and stiff substrates, and the expression levels on the two substrates were similar. The total β1 integrin (including both active and inactive) was higher in hUCMSCs grown on the stiff substrate than that of grown on soft substrates, whereas the activated β1 integrin level on stiff substrates was distinctly lower than that of grown on soft substrates. In conclusion, α5β1 integrin expression in hUCMSCs is dependent on matrix elasticity. The results from this study will provide insight into the role of α5β1 integrin in matrix elasticity-regulated morphologies changes of stem cells and have implication for understanding the mechanism of physical induced lineage specification.

Introduction

Tissue engineering involves functional biomaterial scaffolds and cells for restoring of damaged or diseased tissue. Human umbilical cord-derived mesenchymal stem cells (hUCMSCs) can differentiate into several lineages, including adipose cells, chondrocytes, osteoblasts, neuronal cells, endothelial cells, cardiomyocytes, hepatocyte-like, and pancreatics beta cells [1-3]. hUCMSCs are derived from an ethically uncontroversial and practically inexhaustible source, and may be harvested noninvasively at low cost. Moreover, these cells do not induce teratomas but have anticancer effects [4]. Therefore, hUCMSCs are attractive cells for a multitude of tissue engineering applications.

It is increasingly clear that cells respond to the mechanical properties of their surrounding ECM, including the effects of mechanics on spreading, morphology, and function. Many cell types spread more on stiffer matrix [5, 6] or migrate towards regions of higher modulus [6, 7]. Adhesion [5], tyrosine signaling [8], and proliferation [9, 10] of fibroblasts, smooth muscle cells, and chondrocytes are all regulated by substrate elasticity. Pioneering work on stem cells proved that mesenchymal stem cells (MSCs) cultured on soft matrix (0.1–1 kPa) mimicking the elasticity of

brain became neuronal-like. On a harder matrix (8–17 kPa) mimicking the characteristics of muscle, these stem cells developed myogenic properties, whereas in presence of the hardest matrix (25–40 kPa) mimicking pre-mineralized bone, the cells committed to an osteoblast phenotype [11]. However, the mechanism of mechanotransduction of stem cells is still vague to date.

MSCs interact with ECM predominantly through integrins, heterodimeric adhesion receptors for matrix proteins consisting of α- and β-subunits [12, 13]. Integrins direct inside-out and outside-in signaling that modulates numerous cellular responses, including survival, growth, migration, and differentiation [14]. Different integrins have variable binding affinities for ECM proteins and play distinct roles in cellular mechanosensing. For instance, β3 integrin involves in mechanosensing during matrix elasticity-induced myogenic differentiation of MSCs [15], while α2 integrin modulates MSCs osteogenic differentiation regulated by matrix elasticity [16]. The α5β1 integrin is a specific cell surface receptor for fibronectin that can be found in different adhesion structures [17], and has been implicated in the regulation of differentiation of various cell types, such as precursor cell osteogenic differentiation [18, 19]. However, its effect on MSCs has not been well understood [20]. It has been shown that cellular responsiveness to matrix elasticity is caused by the switch between relaxed and tensioned states of the α5β1 integrin that subsequently activate intracellular signaling cascades and adhesion-dependent motility [21]. Moreover, α5 or β1 integrin subunit and the downstream ERK1/2 signaling have been shown to mediate osteogenic differentiation of MSCs [22, 23]. We suspect that MSCs feel and respond to matrix elasticity through α5β1 integrin. Here, we employed fibronectin coated polyacrylamide substrates of variable elasticity to mimic the physical microenvironment of stem cells. The purpose of this study is to investigate how α5β1 integrin expression changes when hUCMSCs response to matrix elasticity with morphological changes.

Materials and Methods

Isolation, culture and characterization of hUCMSCs. Umbilical cord tissue was obtained from full-term newborn infants delivered by cesarean section at the Norman Bethune 1st Hospital of Jilin University with the Clinical Hospital Ethics Committee approval and written informed consent from newborn's parent. After the delivery of the baby, the umbilical cord is collected and stored in a sterile specimen cup containing 0.9% normal saline at 4 C° until processing. The cord was rinsed several times with sterile phosphate -buffered saline (PBS) to remove residual blood and was cut into 3-5 cm long pieces. Next, blood vessels were removed from each piece after incising the cord lengthwise. The remaining tissue is rinsed. Each piece was then finely chopped and the cord pieces (1–2 mm^3) were place into a sterile 15 ml centrifuge tube and incubated in 3 ml of Collagenase Type Ⅱ (300 units/ml; Gibco, USA) for 14 hours at 37 °C, 5% CO_2. After 14hours, solutions were divided into four equal volumes and diluted with PBS. Each tube was centrifuged at 1500 rmp for 10 minutes. The supernatant was discarded, followed by addition of 10 ml of PBS. Solutions were combined from each tube after centrifuging each tube at 1500 rmp for 5 minuets. The supernatant was discarded and 2 ml of dulbecco's modified eagle medium: nutrient mixture F-12 (DMEM/F-12; Gibco) (plus 10% FBS, 100 U/L penicillin, and 100 mg/L streptomycin) (Beijing Dingguo Changsheng Biotechnology, China) was added to the cell pellet. Cells were resuspended in medium by trituration with a 1000 ml pipette tip. The cells were plated in a 6-well tissue culture plate at a concentration of 30,000 cells per cm^2 and incubated at 37 °C, 5% CO_2 for 48 hours. After 48 hours, the medium was half replaced. Thereafter, the cells were fed by the replacement of half the medium every 2–3 days for expansion. After three passages, hUCMSCs were harvested and subjected to flow cytometry analysis of surface marker expression to confirm the undifferentiated state. The ability to differentiate into mesenchymal lineages, including osteoblasts and adipocytes, was confirmed before these cells were used for further experiments. The adipogenic differentiation of hUCMSCs was induced by in minimum essential medium-a (aMEM) containing 10% fetal bovine serum (FBS), insulin (10 mg/ml), dexamethasone (1 mM) and isobutylxanthine (0.5 mM) (Sigma-Aldrich, USA). To induce osteogenic differentiation, we treated cells with osteogenic medium, and the medium was changed twice per week. Osteogenic medium consists of medium

supplemented with 0.1 mM dexamethasone (Sigma-Aldrich), 10 mM b-glycerol phosphate (Sigma-Aldrich), and 0.2 mM ascorbic acid (Sigma-Aldrich).

Flow cytometric analysis. Expression of surface markers of hUCMSCs was preformed using flow cytometry. Cells were incubated with 10 mg/ml of anti-CD90 (Millipore, USA), CD34 (BD Biosciences, USA), CD37 (BD Biosciences), CD44 (eBioscience, USA), or CD45 (eBioscience) monoclonal antibodies separately for 1 hour at room temperature, and then were analyzed using a FACSCanto II flow cytometer.

Oil red O and alizarin red S staining. For evaluation of lipid droplets, cells were fixed with 4% paraformaldehyde for 15 minutes and stained with 0.375% of oil red O (Sigma-Aldrich) for 20 minutes at room temperature. For characterization of mineralized matrix, cells were fixed with 4% paraformaldehyde and stained with 1% of alizarin red S solution in water for 20 minutes at room temperature.

Growth curves. The cells isolated from umbilical cord tissue were seeded in 24-well plates (0.5×10^4/well). The number of the cells per well were counted every day for 8 successive days.

Fabrication and functionalization of polyacrylamide substrates. Polyacryalmide substrates with tunable mechanical properties were prepared according to Wang and Pelham protocol [24]. Briefly, round glass coverslips were treated with 3‑aminopropyltrimethoxysilane and 0.5% glutaraldehyde. Solutions of 40% acrylamide (Beijing Dingguo Changsheng Biotechnology) and varying concentrations of bis-acrylamide (0.1%, 0.3%, 0.5%, and 0.7%; Amresco, USA) were combined to polymerize to form a layer of gel on the slides. Then 0.25 mM N-sulfosuccinyimidyl-6-(4'-azido-2'-nitrophenylamino) hexanoate (sulfo-SANPAH; Thermo Scientific, USA) dissolved in 50mM HEPES (pH=8.5; Beijing Dingguo Changsheng Biotechnology) and 0.5% dimethylsulfoxide (DMSO; Beijing Dingguo Changsheng Biotechnology) was covered over the polyacrylamide gels and exposed to 365 nm ultraviolet light for 70 minutes for photoactivation in 24-well plates. After being exposed to 253.7 nm ultraviolet light for 30 minutes two times in a row, the polyacrylamide sheet was washed three times with PBS to remove excess reagent and incubated with 200 μl fibronectin solution (1 $\mu g/cm^2$; Sigma-Aldrich) each well overnight at 4 °C. Before cells were plated, the polyacrylamide substrates were soaked in PBS and then in DMEM at room temperature. The compressive Young's modulus of the gels was characterized by a biomechanical testing machine under contact load at a strain rate of 0.5 mm/s.

Morphological changes of the hUCMSCs on substrate with different elasticity. hUCMSCs were plated at 5.0×10^3 cells/cm^2 on four different stiffness polyacrylamide gels (3, 15, 50, and 65 kPa), and each group had three parallel subgroups. Afterwards their morphologic changes were observed and taken photos by inverted phase contrast microscope at 4 hours, 24 hours, 96 hours, 1 week, and 2 weeks after cell inoculation. The major and minor axes of the cell were computed from the moments up to the second order of the thresholded binary image of the cell using the ImageJ software; the cell aspect ratio is the ratio of major to minor axis.

Immunofluorescence staining. hUCMSCs were cultured on polyacrylamide gel-coated plates**.** The cells were fixed in 4% paraformaldehyde for 10 minutes at room temperature, rinsed three times with PBS, and then permeabilized in 0.1% Triton X-100 in PBS for 20 minutes at room temperature. After three rinses with PBS, the plates were incubated with the primary antibodies in PBS containing 1% bovine serum albumin (BSA; Sigma-Aldrich) including anti-rabbit α5 integrin (Millipore), anti-mouse activated β1 integrin (Millipore), anti-mouse total integrin β1 (Millipore), or anti-GAPDH (Millipore), and then with anti-mouse IgG conjugated with Alexa Fluor-488 (Cell Signaling, USA), anti-mouse IgG conjugated with Alexa Fluor-555 (Cell Signaling), or anti-rabbit IgG conjugated with Alexa Fluor-555 (Cell Signaling). Finally, cell nuclei were visualized by Hoechst (Beijing Dingguo Changsheng Biotechnology) and viewed under a microscopy system. Percentages of α5, total β1 integrin positive cells and the ratio of activated β1 integrin to total β1 integrin positive cells were determined by ImageJ analysis.

Statistical analysis. Data from all experiments were expressed as mean ± standard deviation (SD). Unpaired Student's *t*-test was used to compare two set of date, and differences between more than two data sets were determined by one-way ANOVA. $P < 0.05$ was considered significant.

Results

Morphology and immunological phenotype. After the primary culture period (3 days), hUCMSCs were observed to adhere to plastic surfaces and presented a small population of single cells with the edges spreading out (Fig. 1A). On days 7-8 after initial plating, the cells displayed long spindle-shaped fibroblastic cells with obviously large nucleus and abundant cytoplasm (Fig. 1B). When reaching 80% confluence, cells principally formed bipolar spindle-like cells, in parallel or whirlpool-like arrangements after 13-15 days of primary culture (Fig. 1C). One passage of the cell took about 4-6 days. After the cells were continually passaged for a long process, the fibroblast-like cells still retained polygonal or spindly shapes. The cells were considered normal on the basis of typical morphology. Flow cytometry analysis showed that the hUCMSCs at passage 4 were strongly positive for CD105, CD73, CD90, and CD44, but negative for CD34, CD31, and CD45 (Fig. 1D).

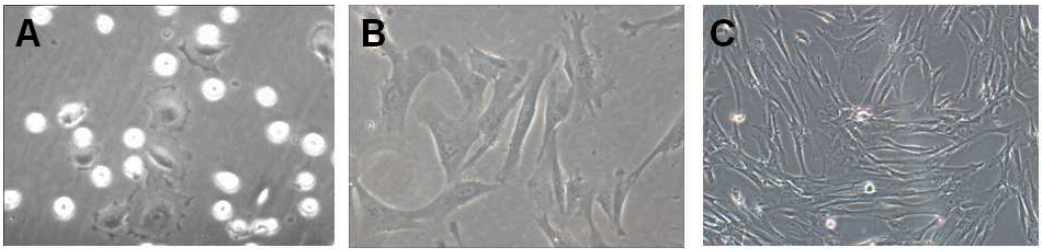

D

Common name	CD locus	Detection
Ecto-5'-nucleotidase (SH3)	CD73	+
Hyaluronan receptor	CD44	+
Thymus cell antigen (Thy-1)	CD90	+
Leukocyte common antigen	CD45	–
Hemopoietic stem cell marker	CD34	–

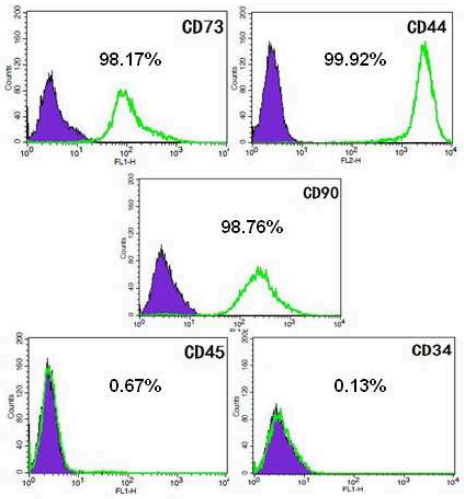

Fig. 1 Morphology and immunological phenotype of hUCMSCs

Fig. 1 is the morphology and immunological phenotype of hUCMSCs. Fig. 1A: The freshly isolated cells from umbilical cord presented a small population of single cells with the edges spreading out. Fig.1B: The cells displayed long spindle-shaped fibroblastic cells with obviously large nucleus and abundant cytoplasm on days 7 after initial primary culture. Fig.1C: On reaching 80% confluence, the primary cells principally formed bipolar spindle-like cells with parallel or whirlpool-like arrangement. Fig.1D: Cell surface marker identification of hUCMSCs. FACS analysis revealed that the 4th passage of hUCMSCs exhibited CD73+, CD44+, CD90+, CD45-, CD34-phenotype.

Growth characteristic and multi-lineage differentiation potential. The growth curve for hUCMSCs showed an 'S' type (Fig. 2). After re-seeding, the cells had 1 day in an adaptive phase. Then, the cells began to expand rapidly and to move into the logarithmic phase of growth. 7 days later, cell counts reached their highest level, followed by a plateau phase. The isolated hUCMSCs displayed the potential to differentiate along adipogenic and osteogenic lineages after treatment with the respective differentiation protocols described in Materials and Methods (Fig. 3). Dense cell packing and calcium deposits stained by alizarin red S were found in hUCMSCs after 4 weeks of osteogenic induction. Similarly, the cells induced with adipogenic medium contained numerous oil-red-O-positive lipid globules at the end of 2 weeks. These results demonstrate that the hUCMSCs used in the present study were indeed multipotent and responsive to differential stimuli.

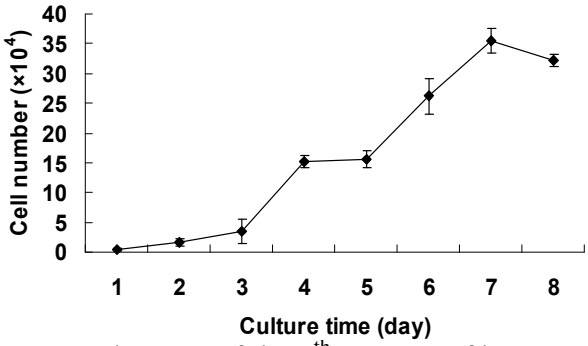

Fig. 2 Growth curve of the 5th passage of hUCMSCs.

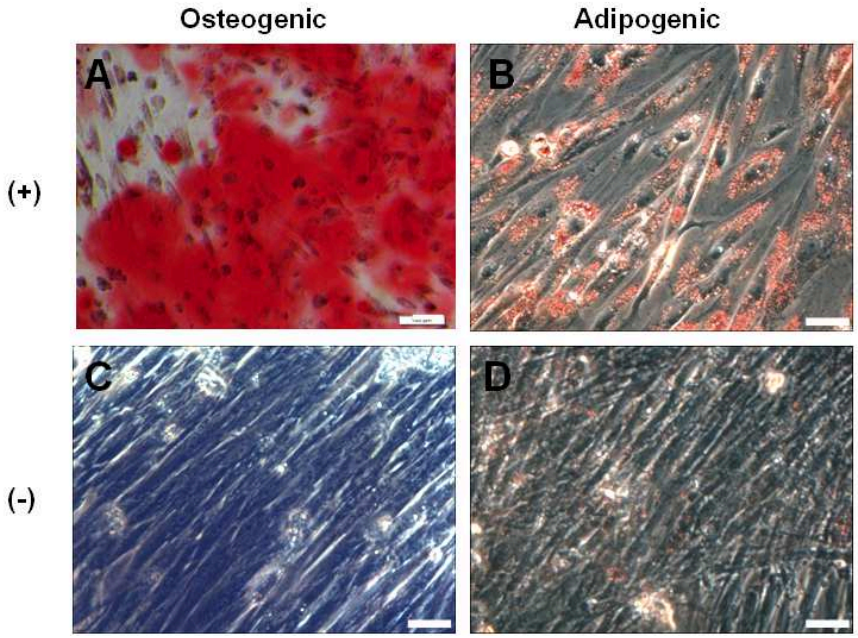

Fig. 3 hUCMSCs after treatment with differentiation protocols

Fig. 3 is hUCMSCs after treatment with differentiation protocols. Fig.3A shows osteogenesis as detected by the formation of calcium deposits stained by alizarin red S after 4 weeks of cultivation. Fig.3B shows adipogenesis as detected by the formation of lipid vacuoles stainable with oil red O after 2 weeks of induction. Fig.3C is non-treated control cultures of osteogenesis. And Fig.3D is non-treated control cultures of adipogenesis. Scale Bar in Fig.3 is 100 μm.

Measurement of substrate elasticity. The mechanical properties of polyacrylamide gels could be easily modified by altering the density of cross-links in the gel. Increasing the concentration of either the amount of acrylamide monomer or bis-acrylamide cross-linker led to a gel with a higher Young's modulus (E) after polymerization. In this way gels of 4 varying stiffness values were obtained as measured by a biomechanical testing machine (Fig. 4).

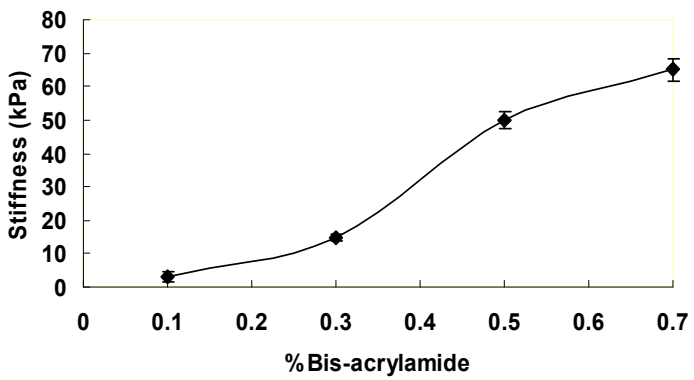

Fig. 4 Stiffness of polyacrylamide gels using 8% acrylamide and different bis-acrylamide concentrations.

Morphological changes of the hUCMSCs on substrates with different elasticity. On polyacrylamide gels with elasticity of 3 kPa, long spindle-shaped cells gradually changed to oval and short spindle shapes with some pseudopodias growth after 4 hours of inoculation. With the extension of pseudopodia, the cells led to branched morphology similar to that of nerve cells by the end of 2 weeks (Fig. 5A). The cells did not show any significant changes in morphology but still remained spindle shape in shape to myoblasts even after 2 weeks on matrices with stiffness of 15 kPa and 50 kPa (Fig. 5A). On the 65 kPa substrate, the pseudopodias of cells stretched out and led to triangular forms after 4 hours. Then not only the spreading area became large but also the quantity of pseudopodias increased. 1 week later, the cells exhibited affluent pseudopodias and showed polygonal shapes similar in morphology to osteoblasts (Fig. 5A).

With the passage of time, hUCMSCs morphology changed distinctly dependent on substrate elasticity (Fig. 5A). After 4 hours of seeding, cells presented spindle shapes at 3, 15, and 50 kPa, whereas hUCMSCs showed unspread and triangular forms. 24 hours later, some slender pseudopodias began to grow on the softest substrates, while lager pseudopodias were observed at both ends of cells on 15 and 50 kPa matrices; hUCMSCs became more spread with cell edges extending around on the stiffest substrates. By the end of 2 weeks, cells obtained branched shapes on 3 kPa matrix and a more stretched or elongated shape appeared at 15 and 50 kPa, while hUCMSCs developed polygonal shapes with large spreading areas. These morphological changes were further confirmed by measuring aspect ratios of cells on different substrates (Fig. 5B).

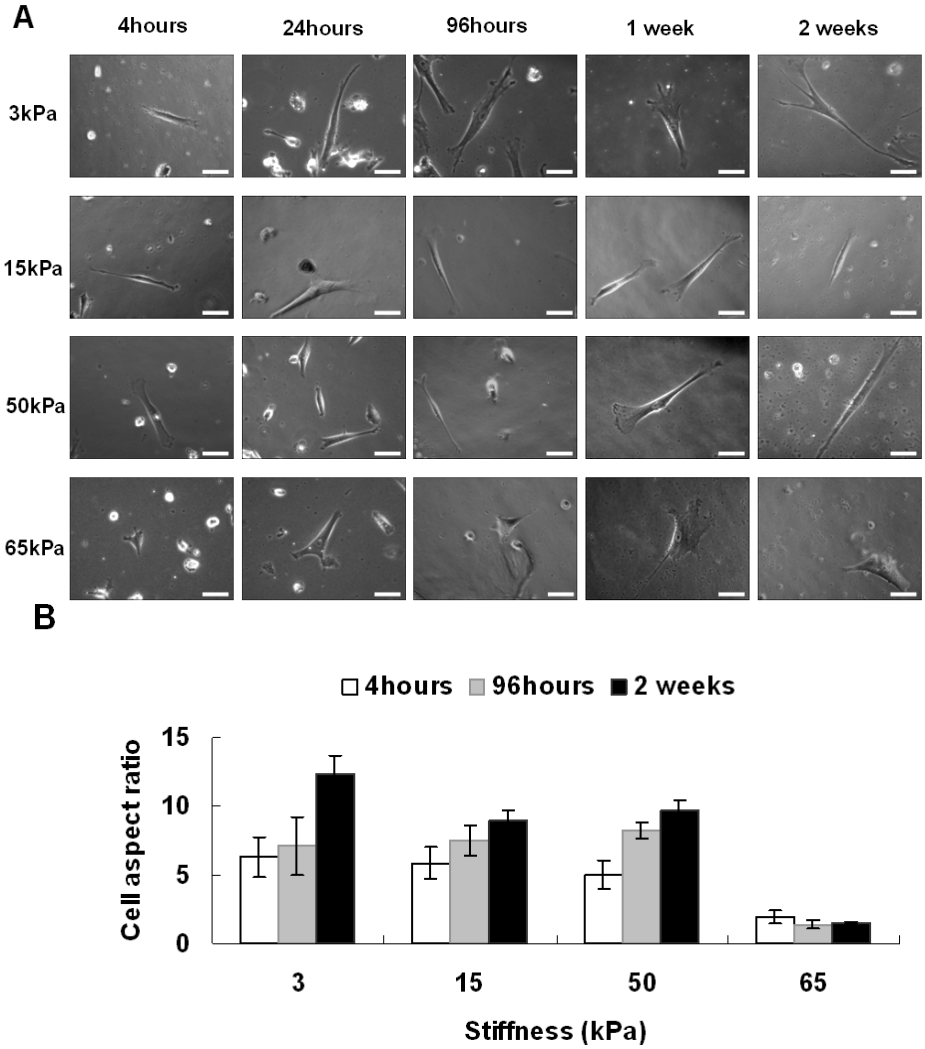

Fig. 5 Morphological changes of the hUCMSCs on substrate with different elasticity. A: hUCMSCs displayed branched or polygonal shapes when grown on matrices of 3 or 65 kPa, and they developed long spindle morphology at 15 and 50 kPa. Scale bar: 20 μm. B: Quantified morphological changes versus stiffness. Cell aspect ratio has significantly different from a variety of stiffness.

α5β1 integrin expression on substrates with different elasticity. hUCMSCs were seeded on fibronectin-coated polyacrylamide gels with two levels of elasticity (E=3 and 65 kPa). The levels of α5β1 integrin were measured 1 week after seeding by Immunofluorescence staining (Fig. 6). We found that hUCMSCs expressed α5 integrin both on soft substrates and stiff substrates, and the expression levels on the two substrates were similar. The total β1 integrin (both active and inactive) was higher in hUCMSCs grown on the 65 kPa substrate than the 3 kPa substrates. In contrast, the activated β1 integrin level on stiff substrate was distinctly lower than that on soft substrate.

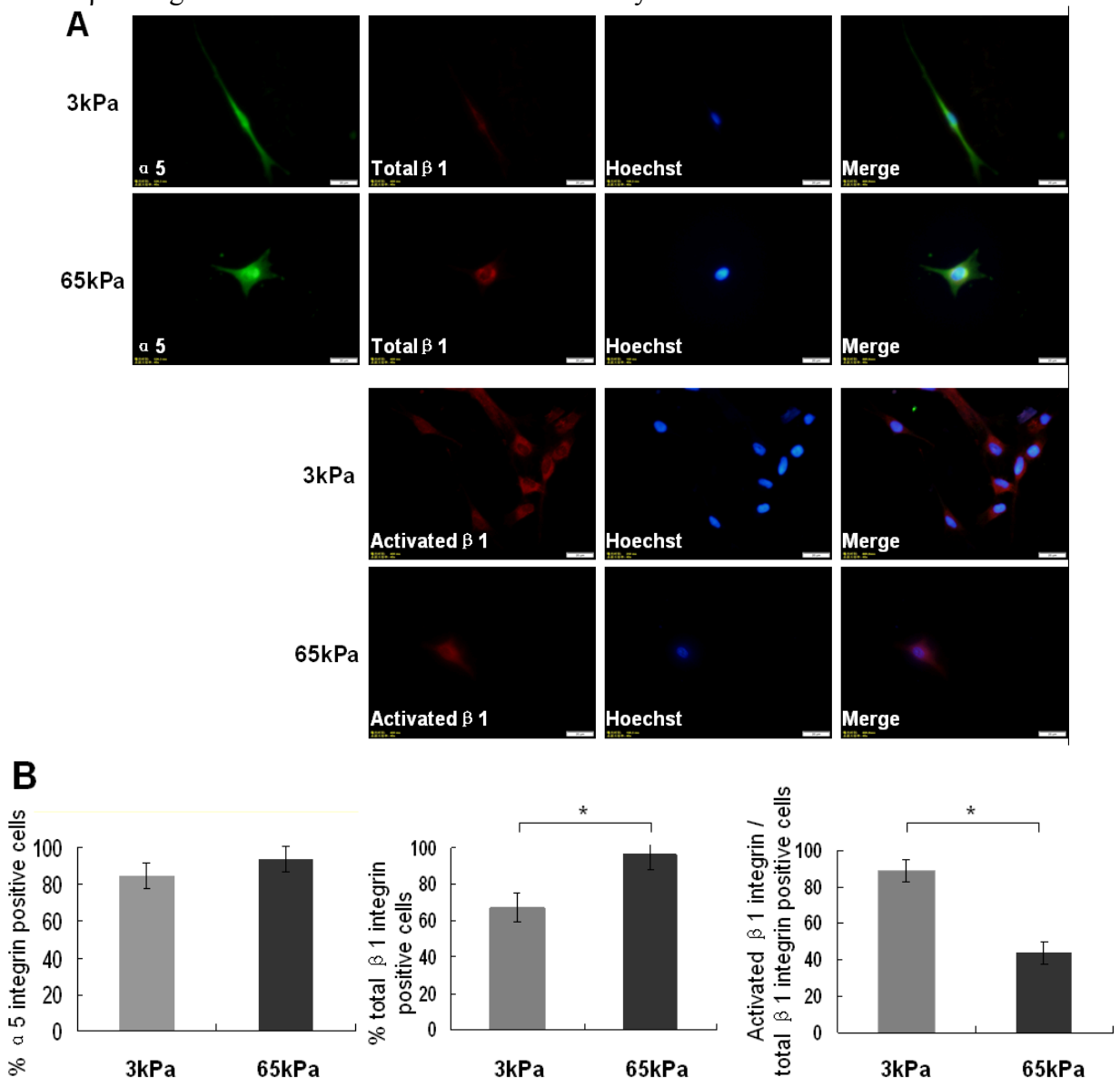

Fig. 6 α5β1 integrin expression changes on substrates of varying elasticity. A: Immunocytochemical staining of α5 integrin, activated, and total β1 integrin levels in hUCMSCs 1 week after seeding on 3 or 65 kPa substrate. Scale bar: 20 μm. B: Percentages of α5, total β1 integrin positive cells and the ratio of activated β1 integrin to total β1 integrin positive cells were measured using ImageJ software. * indicates significant difference ($P < 0.05$).

Discussion

We used in vitro polyacrylamide system as an analogue of the ECM since it has several attractive properties: its elastic modulus can be adjusted precisely by varying the concentrations of acrylamide and bis-acrylamide [24]; its elasticity can be tuned within the physiologically relevant regime from several hundred pascals (brain) to thousands of kilopascals (arties) [24]; altering the mechanical properties does not change the surface chemistry properties [24, 25]; the gel's porosity makes the flow of medium possible, providing a more natural environment than do conventional culture models, such as glass or plastic substrates [26]; adhesive proteins that are covalently attached to the

gel's surface are primary ligands for cell attachment because nonspecific binding of proteins are negligible [27]. The ECM protein fibronectin, whose major ligand is α5β1 integrin, was selected for binding on polyacrylamide hydrogel to improve cell adhesion in this study. The homogeneous fibronectin coating of substrates with variable elasticity will also minimize the influence of surface microstructural cues such as topography and roughness, which may be altered by substrate elasticity modified via hydrogel density. Therefore, fibronectin coated polyacrylamide hydrogel is an appropriate culture platform for studying cell's response to matrix elasticity.

In agreement with other studies [11, 28], we demonstrated that hUCMSCs adopted different morphologies in response to varying substrate elasticity (Fig. 5). Notably, increased cell spreading was associated with increasing stiffness. MSCs on soft matrices of 3 kPa led to branched morphology similar to that of nerve cells; MSCs on medium substrate of 15 kPa presented spindle-shape; polygonal shapes similar to osteoblasts in morphology were detected on stiff substrates (Fig. 5). However, the stiffness of 50 kPa comparable to that of pre-mineralized bone (>30 kPa) induced spindle-shaped cells similar in morphology to myoblasts, in contrast to Engler's work showing that MSCs underwent osteogenesis at 25-40 kPa, while intermediate polyacrylamide gels of 8-17 kPa favored myogenic differentiation [11]. This phenomenon may be attributable to two reasons. First, synthetic matrix materials with the same crosslinking degrees can have distinct modulus due to lack of unified effective representation and measuring methods. Alternatively, different protein coatings to improve cell-adhesive properties or biochemical compositions of matrix used in studies may interact with matrix stiffness and modify the optimal modulus that is determined by stiffness alone for stem cell fate [29, 30]. Cell shape has been shown to regulate cell commitment. McBeath et al. [31] utilized a micropatterning technique to control MSCs shapes and demonstrated that flatten, spread cells differentiated into osteoblasts, while unspread, round cell developed into adipocytes. Furthermore, it was found that the shape-dependent control of stem cell differentiation was mediated by actin-myosin-generated tension through Rho signaling [32, 33]. Thus, while these outputs are not necessarily indicative of stem cell differentiation, morphology can be determinants and effectors of differentiation in both 2D and 3D microenvironments [29, 34].

In this study, we found that hUCMSCs on stiff substrate, displaying polygonal shapes similar in morphology to osteoblasts, expressed up-regulated α5 integrin (Fig. 6). Thus, it is likely that matrix elasticity-driven osteogenic differentiation in hUCMSCs is also associated with α5 integrin similar to biochemical induction. Hamidouche et al. [23, 35] have demonstrated that dexamethasone induced osteogenic commitment in hMSCs is regulated by α5 integrin, as evidenced by reduction of osteogenic specific markers depend upon silencing α5 integrin expression with siRNA. Also, hMSCs developed into osteoblasts upon forced expression of α5 integrin in the absence of dexamethasone, [35] further demonstrating the importance of the α5 integrin-mediated signaling pathway in MSCs osteogenic differentiation. Similarly, integrin α5 expression in MSCs mediated by lentiviral promotes osteogenesis [36]. Surprisingly, MSCs also expressed α5 integrin when cultured on soft substrate with a stiffness of 3 kPa that favors branched morphology (Fig. 6) and prefers neurogenic differentiation [11, 37]. Although the role of α5 integrin in neurogenesis is still unclear to date, α5 subunit is essential for proliferation and survival of cranial neural crest [38] and Schwann cells [39] on fibronectin. Additionally, cardiac neural crest cell and MSCs migrations are modulated by α5β1 integrin-mediated adhesion to fibronectin [40]. Based on these evidences, we could speculate that up-regulated α5 integrin may play a role in hUCMSCs survival or migration. In fact, MSCs tend to migrate to stiffer region of substrate with stiffness gradient. Tse and Engler [41] demonstrated that most MSCs cultured on substrates with a stiffness variation of 1 to 12 kPa migrated to stiffer region and then developed into a more contractile myogenic lineage with elevated expression of myogenic gene, while some cells still showed expression of neural transcript. However, whether α5β1 integrin has an impact on MSCs migration or neurogenic commitment regulated by matrix elasticity needs future study.

Furthermore, we found that expressions of total β1 integrin and activated β1 integrin in hUCMSCs were different between soft substrate and stiff substrate. Total β1 integrin was higher on the 65 kPa substrate in comparison to that on the 3 kPa substrate, while activated β1 integrin level at

65 kPa was distinctly lower than that at 3 kPa (Fig. 6). These findings imply that activated β1 integrin may play a role on soft substrate which induced neuron's morphology (Fig. 5) and is known to regulate neurogenic differentiation, while total β1 integrin may involve in osteogenesis of MSCs induced by stiff matrix, as indicated by cells presenting osteoblast's morphology (Fig. 5). In a study by Du et al [42], soft substrates led to a substantial increase in activation degree and a reduction in cell surface distribution of β1 integrin in MSCs by enhancing the detachment of integrin-ECM protein complexes, which in turn drove activated integrin internalization through caveolae/raft-dependent endocytosis. The enhanced uptake of β1 integrin subsequently blocked the bone morphogenetic protein (BMP)/Smad signal pathway and ultimately led to neural lineage commitment of MSCs. However, BMP/Smad signaling is known to regulate osteogenic differentiation and BMP may work together with matrix stiffness and determine MSC fate [43]. Therefore, activated β1 integrin facilitates neurogenic differentiation on soft substrate, whereas it suppresses osteogenesis on stiff substrate via blocking of BMP/Smad signaling. This may explain why activated β1 integrin was higher on soft matrices than that on stiff matrix in our study (Fig. 6). Nevertheless, β1 integrin has been shown to regulate MSCs osteogenesis induced by ECM or mechanical force. It was found that osteoblast differentiation was induced by the aggregation of cell surface α2β1 integrin with ECM [44], an event triggered by the activation of integrins. More recently, it was found that β1 integrin acted as mechanoreceptors in the mechanotransduction of fluid shear stress in hMSCs during osteogenic differentiation [22]. Although the protein level of integrins has no direct relationship with the integrin signaling pathway, the protein level of integrins determines their distribution in the cytomembrane. Matrix elasticity-induced up-regulation of β1 integrin can result in an increase of β1 integrin distribution in the cytomembrane and accordingly enhance the connection between β1 integrin and ECM. Thus, up-regulation of total β1 integrins on stiff substrate can reinforce the sensing of β1 integrins to higher matrix elasticity.

Conclusions

In summary, hUCMSCs displayed different morphologies in response to the change of matrix elasticity changes, whilst α5β1 integrin expression in hUCMSCs is dependent on matrix elasticity. These studies provide insight into the role of α5β1 integrin in morphological changes of MSCs in response to matrix elasticity and have important implications for the design of biomaterials with appropriate physical property for tissue engineering and regenerative medicine applications.

Acknowledgments

This work was supported by the State Key Development Program for Basic Research of China (Grant No. 2011CB606201), the National Natural Science Foundation of China (Grant No. 31150007, 31201052), China Postdoctoral Science Foundation (Grant No. 20090450415 and 201003125), Bethune Medical Research Support Program-Advanced Interdisciplinary Innovation Project (Grant No. 2013101004), and the Youth Technology Innovation Fund of Jilin University (Grant No. 450060487413).

References

[1] R. Anzalone, M. Lo Iacono, S. Corrao, F. Magno, T. Loria, F. Cappello, G. Zummo, F. Farina, G. La Rocca, New Emerging Potentials for Human Wharton's Jelly Mesenchymal Stem Cells: Immunological Features and Hepatocyte-Like Differentiative Capacity, Stem Cells Dev. 19 (2010) 423-438.

[2] R. Anzalone, M. Lo Iacono, T, Loria, A, Di Stefano, P, Giannuzzi, F, Farina, G, La Rocca, Wharton's Jelly Mesenchymal Stem Cells as Candidates for Beta Cells Regeneration: Extending the Differentiative and Immunomodulatory Benefits of Adult Mesenchymal Stem Cells for the Treatment of Type 1 Diabetes, Stem Cell Rev Rep. 7(2011)342-363.

[3] H.S. Wang, S.C. Hung, S.T. Peng, C.C. Huang, H.M. Wei, Y.J. Guo, Y.S. Fu, M.C. Lai, C.C. Chen, Mesenchymal stem cells in the Wharton's jelly of the human umbilical cord, Stem Cells. 22(2004) 1330-1337.

[4] M. Witkowska-Zimny, E. Wrobel, Perinatal sources of mesenchymal stem cells: Wharton's jelly, amnion and chorion, Cell Mol Biol Lett. 16(2011) 493-514.

[5] T. Yeung, P.C. Georges, L.A. Flanagan, B. Marg, M. Ortiz, M. Funaki, N. Zahir, W.Y. Ming, V. Weaver, P.A. Janmey, Effects of substrate stiffness on cell morphology, cytoskeletal structure, and adhesion, Cell Motil Cytoskel. 60(2005) 24-34.

[6] C.M. Lo, H.B. Wang, M. Dembo, Y.L. Wang, Cell movement is guided by the rigidity of the substrate, Biophysical Journal. 79(2000) 144-152.

[7] J.T. Smith, J.T. Elkin, W.M. Reichert, Directed cell migration on fibronectin gradients: Effect of gradient slope, Exp Cell Res. 312(2006) 2424-2432.

[8] G. Giannone, M.P. Sheetz, Substrate rigidity and force define form through tyrosine phosphatase and kinase pathways, Trends in cell biology. 16(2006) 213-223.

[9] A. Subramanian, H.Y. Lin, Crosslinked chitosan: Its physical properties and the effects of matrix stiffness on chondrocyte cell morphology and proliferation, Journal of Biomedical Materials Research Part A. 75A(2005) 742-753.

[10] S.R. Peyton, C.B. Raub, V.P. Keschrumrus, A.J. Putnam, The use of poly(ethylene glycol) hydrogels to investigate the impact of ECM chemistry and mechanics on smooth muscle cells, Biomaterials. 27(2006) 4881-4893.

[11] A.J. Engler, S. Sen, H.L. Sweeney, D.E. Discher, Matrix elasticity directs stem cell lineage specification, Cell. 126(2006) 677-689.

[12] C.H. Damsky, D. Ilic, Integrin signaling: it's where the action is, Curr Opin Cell Biol. 14(2002) 594-602.

[13] R.O. Hynes, Integrins: Bidirectional, allosteric signaling machines, Cell. 110(2002) 673-687.

[14] E.H.J. Danen, A. Sonnenberg, Integrins in regulation of tissue development and function, J Pathol. 200(2003) 471-480.

[15] H.Y. Yu, Y.S. Lui, S.J. Xiong, W.S. Leong, F. Wen, H. Nurkahfianto, S. Rana, D.T. Leong, K.W. Ng, L.P. Tan, Insights into the Role of Focal Adhesion Modulation in Myogenic Differentiation of Human Mesenchymal Stem Cells, Stem Cells Dev. 22(2013) 136-147.

[16] Y.R. Shih, K.F. Tseng, H.Y. Lai, C.H. Lin, O.K. Lee, Matrix stiffness regulation of integrin-mediated mechanotransduction during osteogenic differentiation of human mesenchymal stem cells, J Bone Miner Res. 26(2011) 730-738.

[17] M. Larsen, V.V. Artym, J.A. Green, K.M. Yamada, The matrix reorganized: extracellular matrix remodeling and integrin signaling, Curr Opin Cell Biol. 18(2006) 463-471.

[18] S.N. Stephansson, B.A. Byers, A.J. Garcia, Enhanced expression of the osteoblastic phenotype on substrates that modulate fibronectin conformation and integrin receptor binding, Biomaterials. 23(2002) 2527-2534.

[19] B.G. Keselowsky, L. Wang, Z. Schwartz, A.J. Garcia, B.D. Boyan, Integrin alpha(5) controls osteoblastic proliferation and differentiation responses to titanium substrates presenting different roughness characteristics in a roughness independent manner, Journal of Biomedical Materials Research Part A. 80A (2007) 700-710.

[20] D. Docheva, C. Popov, W. Mutschler, M. Schieker, Human mesenchymal stem cells in contact with their environment: surface characteristics and the integrin system, J Cell Mol Med. 11(2007) 21-38.

[21] J.C. Friedland, M.H. Lee, D. Boettiger, Mechanically Activated Integrin Switch Controls alpha(5)beta(1) Function, Science. 323(2009) 642-644.

[22] L.Y. Liu, C. Zong, B. Li, D. Shen, Z.H. Tang, J.R. Chen, Q. Zheng, X.M. Tong, C.Y. Gao, J.F. Wang, The interaction between beta 1 integrins and ERK1/2 in osteogenic differentiation of human mesenchymal stem cells under fluid shear stress modelled by a perfusion system, J Tissue Eng Regen M. 8(2014) 85-96.

[23] Z. Hamidouche, O. Fromigue, J. Ringe, T. Haupl, P. Vaudin, J.C. Pages, S. Srouji, E. Livne, P.J. Marie, Priming integrin alpha5 promotes human mesenchymal stromal cell osteoblast differentiation and osteogenesis, Proc Natl Acad Sci U S A. 106(2009) 18587-18591.

[24] R.J. Pelham, Jr., Y. Wang, Cell locomotion and focal adhesions are regulated by substrate flexibility. Proc Natl Acad Sci U S A, 94(1997) 13661-13665.

[25] K. Lee, Q.K. Chen, C. Lui, M.A. Cichon, D.C. Radisky, C.M. Nelson, Matrix compliance regulates Rac1b localization, NADPH oxidase assembly, and epithelial-mesenchymal transition, Mol Biol Cell. 23(2012) 4097-4108.

[26] Y.L. Wang, R.J. Pelham, Jr., Preparation of a flexible, porous polyacrylamide substrate for mechanical studies of cultured cells, Methods Enzymol. 298(1998) 489-496.

[27] C.E. Kandow, P.C. Georges, P.A. Janmey, K.A. Beningo, Polyacrylamide hydrogels for cell mechanics: steps toward optimization and alternative uses, Methods Cell Biol. 83(2007) 29-46.

[28] K. Ghosh, Z. Pan, E. Guan, S.R. Ge, Y.J. Liu, T. Nakamura, X.D. Ren, M. Rafailovich, R.A.F. Clark, Cell adaptation to a physiologically relevant ECM mimic with different viscoelastic properties, Biomaterials. 28(2007) 671-679.

[29] A.S. Rowlands, P.A. George, J.J. Cooper-White, Directing osteogenic and myogenic differentiation of MSCs: interplay of stiffness and adhesive ligand presentation, Am J Physiol Cell Physiol. 295(2008) C1037-1044.

[30] J. Lee, A.A. Abdeen, D. Zhang, K.A. Kilian, Directing stem cell fate on hydrogel substrates by controlling cell geometry, matrix mechanics and adhesion ligand composition, Biomaterials. 34(2013) 8140-8148.

[31] R. McBeath, D.M. Pirone, C.M. Nelson, K. Bhadriraju, C.S. Chen, Cell shape, cytoskeletal tension, and RhoA regulate stem cell lineage commitment, Developmental Cell. 6(2004) 483-495.

[32] R.K. Assoian, E.A. Klein, Growth control by intracellular tension and extracellular stiffness, Trends in Cell Biology. 18(2008) 347-352.

[33] A.L. Zajac, D.E. Discher, Cell differentiation through tissue elasticity-coupled, myosin-driven remodeling, Curr Opin Cell Biol. 20(2008) 609-615.

[34] W.A. Comisar, N.H. Kazmers, D.J. Mooney, J.J. Linderman, Engineering RGD nanopatterned hydrogels to control preosteoblast behavior: A combined computational and experimental approach, Biomaterials. 28(2007) 4409-4417.

[35] Z. Hamidouche, O. Fromigue, J. Ringe, T. Haupl, P.J. Marie, Crosstalks between integrin alpha 5 and IGF2/IGFBP2 signalling trigger human bone marrow-derived mesenchymal stromal osteogenic differentiation, Bmc Cell Biol. 11(2010) 44.

[36] S. Srouji, D. Ben-David, O. Fromigue, P. Vaudin, G. Kuhn, R. Muller, E. Livne, P.J. Marie, Lentiviral-Mediated Integrin alpha 5 Expression in Human Adult Mesenchymal Stromal Cells Promotes Bone Repair in Mouse Cranial and Long-Bone Defects, Hum Gene Ther. 23 (2012) 167-172.

[37] M. Lanniel, E. Huq, S. Allen, L. Buttery, P.M. Williams, M.R. Alexander, Substrate induced differentiation of human mesenchymal stem cells on hydrogels with modified surface chemistry and controlled modulus, Soft Matter. 7(2011) 6501-6514.

[38] K.L. Goh, J.T. Yang, R.O. Hynes, Mesodermal defects and cranial neural crest apoptosis in alpha5 integrin-null embryos, Development. 124(1997) 4309-4319.

[39] H. Haack, R.O. Hynes, Integrin receptors are required for cell survival and proliferation during development of the peripheral glial lineage, Dev Biol. 233(2001) 38-55.

[40] A. Mittal, M. Pulina, S.Y. Hou, S. Astrof, Fibronectin and integrin alpha 5 play essential roles in the development of the cardiac neural crest, Mech Develop. 127(2010) 472-484.

[41] J.R. Tse, A.J. Engler, Stiffness Gradients Mimicking In Vivo Tissue Variation Regulate Mesenchymal Stem Cell Fate, Plos One. 6(2011) e15978.

[42] J. Du, X.F. Chen, X.D. Liang, G.Y. Zhang, J. Xu, L.R. He, Q.Y. Zhan, X.Q. Feng, Integrin activation and internalization on soft ECM as a mechanism of induction of stem cell differentiation by ECM elasticity, P Natl Acad Sci USA. 108(2011) 9466-9471.

[43] O.F. Zouani, J. Kalisky, E. Ibarboure, M.C. Durrieu, Effect of BMP-2 from matrices of different stiffnesses for the modulation of stem cell fate, Biomaterials. 34(2013) 2157-2166.

[44] Y. Takeuchi, M. Suzawa, T. Kikuchi, E. Nishida, T. Fujita, T. Matsumoto, Differentiation and transforming growth factor-beta receptor down-regulation by collagen-alpha2beta1 integrin interaction is mediated by focal adhesion kinase and its downstream signals in murine osteoblastic cells, J Biol Chem. 272(1997) 29309-29316.